

An Exploration of Chrysin Fabricated Silver Nanoparticles as Antibiofilm Agent against *Pseudomonas aeruginosa*

Arnica F Lal, Pushpraj S Gupta*

Department of Pharmaceutical Science, SHALOM Institute of Health and Allied Sciences, Sam Higginbottom University of Agriculture, Technology and Sciences, Naini, Prayagraj, Uttar Pradesh, INDIA.

ABSTRACT

Background: *Pseudomonas aeruginosa* (*P. aeruginosa*) is the source of serious nosocomial infections, the most common of which is ventilator-associated pneumonia. *P. aeruginosa* infections continue to pose a substantial therapeutic problem. The expression of several virulence genes and the formation of biofilms in bacteria are caused by quorum sensing, a density-dependent cell-to-cell communication mechanism. Anti-biofilm chemicals prevent the synthesis of the polymer matrix, limit cell adhesion and attachment, reduce the generation of virulence factors, and obstruct the quorum sensing system. The present study focused on the antibiofilm activity of chrysin-fabricated silver nanoparticles (nano-chrysin) against *P. aeruginosa*. **Materials and Methods:** In our study, chrysin, which is a polyphenol, was fabricated with silver nanoparticles to make nano-chrysin. *P. aeruginosa* PAO1 strain was treated at sub-MIC concentrations with chrysin (50, 25, 12.5, and 6.25 $\mu\text{g mL}^{-1}$), silver nanoparticles (6.26, 3.13, 1.56, and 0.78 $\mu\text{g mL}^{-1}$) and formulated nano-chrysin (3.13, 1.56, 0.78, and 0.39 $\mu\text{g mL}^{-1}$) to find out the effectiveness of these compounds against biofilm formation. **Results:** Biofilm produced by *P. aeruginosa* PAO1 was found to be inhibited at sub-MIC concentrations (3.13, 1.56, 0.78, and 0.39 $\mu\text{g mL}^{-1}$) of nano-chrysin having MIC value ranging between 50-3.13 $\mu\text{g mL}^{-1}$ which is more potent than alone chrysin and silver nanoparticles. **Conclusion:** The data confirmed that nano-chrysin is effective in inhibiting biofilm formation, produced by *P. aeruginosa*.

Keywords: Chrysin, Nanoparticle, *P. aeruginosa*, Antibiofilm, Quorum sensing.

INTRODUCTION

Humans become prone to certain infections after surgery; one of the most common infections is caused by *Pseudomonas aeruginosa* (*P. aeruginosa*), particularly in the blood, lungs, and other parts of the body.¹ They live in the environment and are most commonly acquired in healthcare settings, causing much more infections in patients who are especially immunocompromised, on ventilators or catheters, and in patients affected by wounds resulting from surgery and burns.²

Demand for treatment of infections caused by *P. aeruginosa* is on the rise as the strain has developed multi-drug resistance; hence, there is an urgent need for alternative therapies.³

Chrysin (5,7-dihydroxyflavone), is a flavones that is a secondary metabolite found in honey (Apidae), propolis (Salicaceae), *Oroxylum indicum* (Bignoniaceae), the passion flowers, *Passiflora incarnata*, and *Passiflora caerulea* (Passifloraceae).⁴ This dietary

natural product possesses tremendous healing properties against toxic agents in various tissues of the brain, heart, liver, kidney, and lung.⁵ Owing to its great medicinal value, the problem with chrysin is its low bioavailability and poor intestinal absorption. The main causes of poor systemic bioavailability for chrysin include low water solubility, fast metabolism mediated by UGTs (Uridine 5'-diphospho-glucuronosyltransferase) and SULT (Cytosolic Sulfotransferases), and effective excretion through efflux transporters including BCRP (Breast Cancer Resistance Protein) and MRP2 (Multidrug Resistance Protein 2).⁶

The associated problems with chrysin can be overcome by new drug delivery approaches, including articulation into nanoparticles.⁷ Nanoparticles have proven to be an effective small carrier molecule (nanocarrier) over the past decades and have been shown to increase the pharmacokinetic and pharmacodynamic properties of drug molecules.⁸

A biofilm is made up of bacterial cell clusters that have a network of hollows or internal channels in the extracellular polysaccharide and glycoprotein matrix that allow the cells to absorb nutrients and oxygen from the surrounding bulk liquid. Biofilm, thus, is described as a microbiologically formed a stationary community made up of cells that attach to the



DOI: 10.5530/ijper.58.2s.46

Copyright Information:

Copyright Author (s) 2024 Distributed under Creative Commons CC-BY 4.0

Publishing Partner: EManuscript Tech. [www.emanuscript.in]

Extracellular Polymeric Substance (EPS) matrix and embed in it, changing their phenotypic in terms of gene transcription and growth rate.⁹ Because they have a barrier preventing contact with antimicrobial agents, biofilms are more resistant to antimicrobials than bacteria. These serve as a resistance for the host environment as they do not allow the drug to reach the target site due to the dense polymeric cascade network, which hence contributes to the resistance through the Quorum Sensing (QS) signaling mechanism in *P. aeruginosa*.¹⁰ The processes that result in biofilm formation are as follows: (a) cell transport from the surface and bacterial adsorption at the surface; (b) production of EPS and cell-to-cell signaling molecules and irreversible cell adsorption; (c) biofilm maturation; (d) detachment of some biofilm cells; and (e) biofilm recolonization. *P. aeruginosa* biofilm production has been demonstrated to depend on bacterial cell communication.¹¹ The QS bacterial cell-to-cell communication system controls the virulence genes in *P. aeruginosa*.¹² Small signaling molecules made by QS bacteria can interact with related receptors when they are present in large numbers. This connection triggers the expression of several genes involved in bacterial pathogenicity and the development of biofilms.¹²

Polyphenols, which are derived from plants, fight infections. For instance, furocoumarins block the production of biofilms on bacterial strains such as *P. aeruginosa*, *Salmonella typhimurium*, and *Escherichia coli*, as well as AI-1 and AI-2 signaling. Maurobarbaro C. impacts the signaling systems of lasR and rhlR against *P. aeruginosa* and *Chromobacterium violaceum*. Curcumin inhibits the virulence genes expression on *P. aeruginosa*. Urolithins A and B decrease *Yersinia enterocolitica* QS processes and levels. The DNA-binding capacity of the LuxR transcriptional protein of *Vibrio* spp. and *Escherichia coli* is impacted by cinnamaldehyde, which changes the virulence factors, swimming motility, biofilm structure, and stress response.¹³ Quercetin has its many advantages included its ability to suppress the formation of biofilms, block the SrtA gene, and exhibit an effect on the generation of sialic acid in opposition to *Streptococcus pneumoniae*.^{14,15} Additionally, this chemical hinders *P. aeruginosa*'s synthesis of RhlI, RhlR, LasI, and LasR. Polyphenol-encapsulated nanoparticles have proven to treat such resistance and lower the dependency on antibiotics that create antimicrobial resistance over prolonged use.¹⁶

In our study, we have formulated chrysin inclusion silver nanoparticle¹⁷ and tested it on biofilm produced by *P. aeruginosa* PAO1 strain. The results have shown positive inhibition against biofilm formed by the *P. aeruginosa* PAO1 strain. This research is the first to explore the potential of bio-reduced silver nanoparticles through chrysin and their clinical implications on bacterial pathogenesis, like *P. aeruginosa* biofilm formation.

MATERIALS AND METHODS

Materials

Silver nitrate and chrysin were purchased from Sigma Aldrich, India. In this study, *P. aeruginosa* was used as a culture *P. aeruginosa* PAO1 was used as a bacterial strain. Assay plates for antimicrobial activity, MIC, and antibiofilm activity included nutrient broth media, which was purchased from Hi Media Laboratories Pvt. Ltd., India. Ethanol was purchased from Rankem Ltd., India and vancomycin from Sigma Aldrich, India.

Synthesis of nano-chrysin (Chrysin@AgNPs) by Chemical Reduction

Chrysin, a natural reducing agent, is used to reduce the metal ion Ag⁺ to Ag⁰ via the green route without using toxic chemicals. The chrysin and AgNO₃ were mixed at a concentration of 0.5:1 mM with constant stirring at an increasing temperature of 30°C to 90°C.¹⁷ pH was maintained at every time interval with 0.1 N NaCl and 0.1 N HCl, and incubation time was extended up to 90 min to obtain more uniform and smaller NPs. The formation of NPs was confirmed due to SPR absorbance by UV.

Characterization of nano-chrysin

UV (Ultra-Violet analysis)

Based on SPR (Surface Plasmon Resonance), UV-vis is a preliminary method to identify the reduction that the reducing agent made to the metal. A systronic UV-visible spectrophotometer recorded absorbance maxima at the wavelength of 200-800 nm in order to perform UV-vis on the sample.

FTIR (Fourier-Transform Infrared Spectroscopy)

The surface chemistry was studied by the FTIR spectroscopic technique, KBr pellets were mixed with the sample and used after drying. The transmittance was measured by an FTIR spectrometer with a wavelength ranging from 4000 cm⁻¹ to 400 cm⁻¹.

SEM and TEM (Morphological analysis)

The surface morphology of nanoparticles was studied through images obtained with SEM (scanning electron microscopy) using the FEI Nova Nano FESEM 450. A range of kV, at both low (for high-resolution imaging) and high (for microanalytical imaging) currents, is possible with the Schottky field-emission source of the NanoSEM 450. HRTEM (high resolution transmission electron microscope) was carried out using the JEOL JEM 2100 PLUS High-Resolution Transmission Electron Microscope at an accelerating voltage of 200 kV with a resolution point of 0.194 nm and a lattice of 0.14 nm.

XRD (X-ray Diffraction Analysis)

The phase characteristics and dimension of the formulated nanoparticles were determined by the *h*, *k*, and *l* values obtained by the X-ray Diffraction (XRD) technique using Panalytical Xpert Powder. It directly probes the crystallographic structure of nanoparticles and changes in their structure. The mean particle size of nanoparticles was calculated using Debye Scherrer's equation.

$$L = 0.9\lambda/\beta \cosh \theta$$

Where, λ is the wavelength of X-ray, β is full width and half maximum, and θ is the Bragg's angle.

Zeta Potential, Particle size analysis and Polydispersity Index

A zeta potential sizer (-100 mv to +100 mv) measures the electrostatic potential at the electrical double layer surrounding a nanoparticle in solution. It is performed using a clear disposable zeta cell and a Malvern Zeta Potential DTS0050 at 25°C. Particle size analysis can be used to measure the polydispersity index, which indicates the average molecular weight of the particles as measured with the equation,

$$M_w/M_n$$

Where, M_w and M_n are the weight average and number average molecular weight, respectively.

Anti-microbial assay and Minimum Inhibitory Concentration (MIC)

A 20 μ L overnight-grown microbial culture petriplate containing nutrient agar media was covered with a disc of chrysin, silver nanoparticles, and nano-chrysin. The zones of inhibition on the plates were measured in millimetres after 48 hr of incubation at 37°C.¹⁸ A 100 mL portion of sterilized nutrient broth was made, and a bacterial culture was injected into the medium of the broth to determine the MIC. The microtiter plate wells received 200 μ L of broth. A 200 μ L sample dilution was performed. Absorbance was measured in nm after 48 hr of incubation at 37°C.¹⁹

Biofilm inhibition assay

A complex microbial community that is highly resistant to antimicrobial agents is known as a biofilm. Higher levels of mortality and morbidity are associated with the formation of biofilms on biotic and abiotic surfaces. Moreover, it is thought to be a crucial component of bacterial pathogenicity. The bacterial culture was inoculated in the broth medium of 100 mL of sterilized nutrient broth for the antibiofilm experiment. The microtiter plate wells received 200 μ L of broth. Samples comprising 200 μ L were inoculated. 72 hr incubation period at 37°C. Each well's bacterial suspension was gently removed after incubation. To get rid of free-floating planktonic bacteria, the wells were washed

three times with 200 μ L of Phosphate Buffered Saline (PBS). The wells were then left to air dry for 45 min. Crystal violet was used to detect bacterial adhesion to the culture plate. 200 μ L of crystal violet (0.1%) was added to each well, and the plates were cultured at room temperature for 10 min. Plates were left for 20 min to dry after the excess stain was wiped off by washing with deionized water (washed three times with 300 μ L of water). Following drying, 200 μ L of 95% ethanol was poured into each well to dissolve the included dye. The plate was then covered with a lid to prevent evaporation and left at room temperature for 30 min. At 570 nm, the absorbance of the stained adhering bacteria was measured using a microplate reader.²⁰

RESULTS

Synthesis and Characterization of nano-chrysin

UV (Ultra-Violet analysis)

The SPR phenomenon attributed to the dispersity, size, and shape of nanoparticles was confirmed by UV-vis spectrophotometry²¹ with the formation of a yellowish-brown colour. As per (Figure 1) for UV-vis, the wavelength is 420 nm at 90 min.¹⁷

FTIR (Fourier-Transform Infrared Spectroscopy)

In FTIR data (Figure 2a), the free chrysin displays transmittance at 3084, 3011, 2923, 1651, and 1611 cm^{-1} in the infrared spectrum. Strong bands between 3500 and 3000 cm^{-1} are associated with the OH stretch, while 1651 and 1611 cm^{-1} stand for C=O and C=C, respectively. It is abundantly obvious from the distinctive IR transmittance of produced NPs that functional groups of chrysin actively participate in coordination with metal ions.

Differences in the intensity of transmittance at 3500-3000 cm^{-1} seen in the formulated nano-chrysin complex after reduction are a vivid illustration of the symmetrical and asymmetrical stretching modes of O-H (Figure 2b). This variation in intensity implies that one O-H group was involved in coordination with the metal ions.²² The C=O oxygen atom, which was shifted to 1640 cm^{-1} in the spectra of the nano-chrysin complex and therefore is attributed to a strong band at about 1651 cm^{-1} that was identified

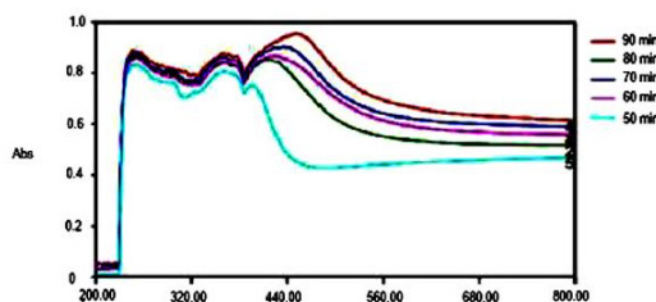


Figure 1: Absorbance graph of formulated nano-chrysin at 50-90 min of interval.

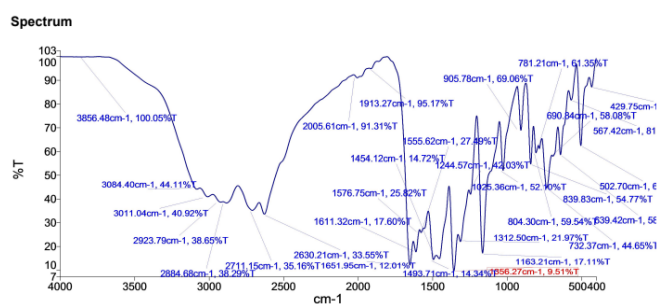


Figure 2a: FTIR data of pure chrysin.

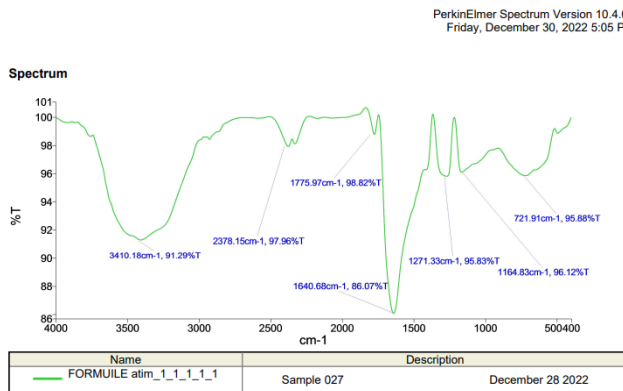


Figure 2b: FTIR data of nano-chrysin.

in the transmittance of the ligand, indicates that the cross-linking of chrysin on metal nanoparticles takes place through the C=O oxygen atom.²³

SEM and TEM (Morphological analysis)

The morphology analysis of SEM (Figure 3a) showed uniform and well dispersed nanoparticles with a spherical shape having a nano-chrysin (Chrysin@AgNPs) mean diameter of around 56 nm that might be influenced by chrysin in formulating AgNPs.

Whereas HRTEM was carried out to look further into the characteristic shape and size of formed NPs. (Figure 3b) depicts insights into the shape and size of NPs, with sizes ranging from 2 to 50 nm. Most NPs were spherical in nature, followed by triangular.

XRD (X-ray Diffraction Analysis)

With the aid of JCPDS intensities, the XRD patterns of nano-chrysin were deciphered. After reduction, the diffraction peaks at $2\theta=29.45$, 31.72 , and 66.25 were indexed as $(1\ 1\ 1)$, $(2\ 0\ 0)$, and $(2\ 2\ 0)$ planes of a faced-centered cubic (fcc) lattice of silver (JCPDS, file no. 04-0783) (Figure 4). The XRD patterns seen here have a thin layer of chrysin coating on the metal surface,¹¹ and well-dispersed particles that remained stable for an extended period of time with a minimum particle size of 2 nm.²⁴

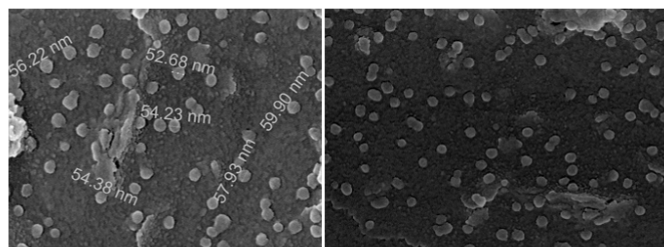


Figure 3a: SEM micrographs of nano-chrysin.

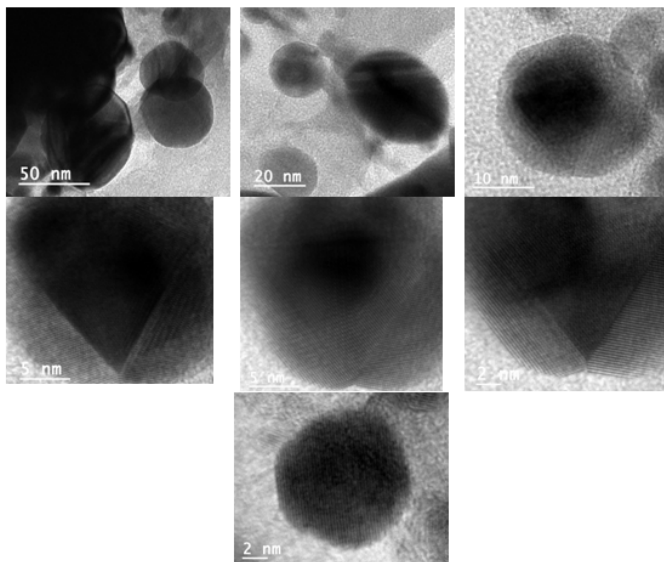


Figure 3b: HRTEM micrographs of nano-chrysin.

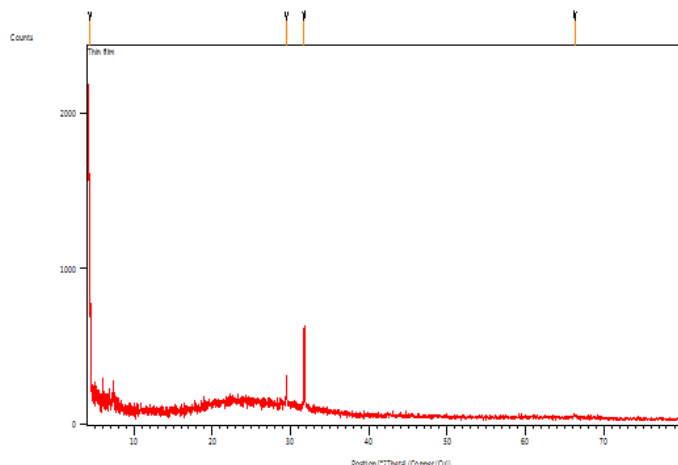


Figure 4: The XRD patterns of nano-chrysin.

Zeta Potential, Particle size and Polydispersity Index

The Polydispersity Index (PDI) indicates the uniform distribution and dispersion of the particles throughout the sample solution to determine whether a sample is homogeneous or heterogeneous. With a range of 0.26 (Table 1) it is evident that $PDI \leq 0.2$ is acceptable for nanomaterial formulation in drug delivery system.²⁵

Antimicrobial assay and MIC

According to the results of the antimicrobial experiment, chrysin, Silver Nanoparticles (AgNPs), and nano-chrysin (Chrysin@AgNPs) all displayed zones of inhibition at a concentrations of 50, 100, 150 and 200 $\mu\text{g mL}^{-1}$, with diameters of 7, 17, 30 and 36 mm for chrysin (Figure 5a), 22, 37, 42 and 47 mm for silver nanoparticles (Figure 5b), and 32, 38, 45 and 49 mm for Chrysin@AgNPs (Figure 5c), respectively, while the positive control vancomycin; exhibited with an 8 mm zone of inhibition at all four concentrations. Vancomycin is considered a standard in antimicrobial susceptibility analysis against *P. aeruginosa*.²⁶ This proves that the inhibitory zone of chrysin, when coupled with silver to generate nano-chrysin, is higher than that of its individual parts at all four concentrations. Chrysin Silver Nanoparticles (AgNPs), and nano-chrysin were each shown to have MICs of 50 $\mu\text{g mL}^{-1}$ at $\text{OD}_{600}=0.009$, 6.25 $\mu\text{g mL}^{-1}$ at $\text{OD}_{600}=0.005$, and 3.13 $\mu\text{g mL}^{-1}$ at $\text{OD}_{600}=0.024$, respectively, demonstrating nano-chrysin potency and efficacy in comparison to chrysin and AgNPs.

Antibiofilm assay

The virulence feature of *P. aeruginosa*, which is created via intricate gene regulation in the Las system, is shown by the creation of biofilms.²⁷ In our study, it is evident that chrysin, when fabricated with silver nanoparticles forming nano-chrysin, shows better potency and efficacy in inhibiting biofilm formation with

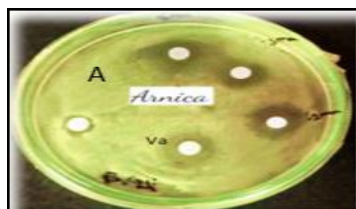


Figure 5a: Zone of inhibition formed by chrysin at 50, 100, 150 and 200 $\mu\text{g mL}^{-1}$, Vancomycin (+ve, positive control).



Figure 5b: Zone of inhibition formed by Silver Nanoparticles (AgNPs) at 50, 100, 150 and 200 $\mu\text{g mL}^{-1}$, Vancomycin (+ve, positive control).

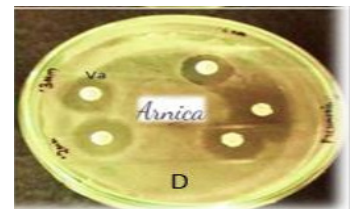


Figure 5c: Zone of inhibition formed by nano-chrysin (Chrysin@AgNPs) at 50, 100, 150 and 200 $\mu\text{g mL}^{-1}$, Vancomycin (+ve, positive control).

Table 1: Polydispersity index of formulated nano-chrysin.

Z-Average (d.nm)	3837
PDI	0.265
Intercept	0.813

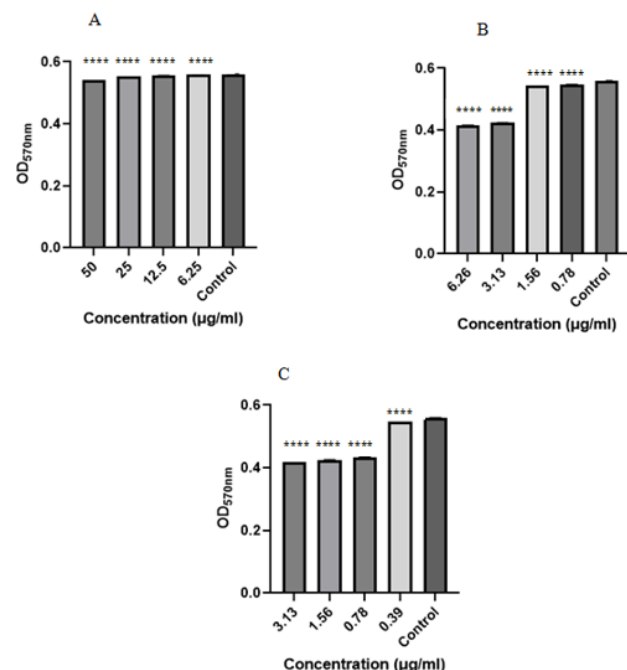


Figure 6: Graph depicting antibiofilm activity of chrysin (A), silver nanoparticle (B), nano-chrysin (Chrysin@AgNPs) (C) against *P. aeruginosa* were quantified through OD_{570} after 48 hr of incubation. Error bars indicate the standard deviation in triplicate. ****, $p<0.05$ compared with the control.

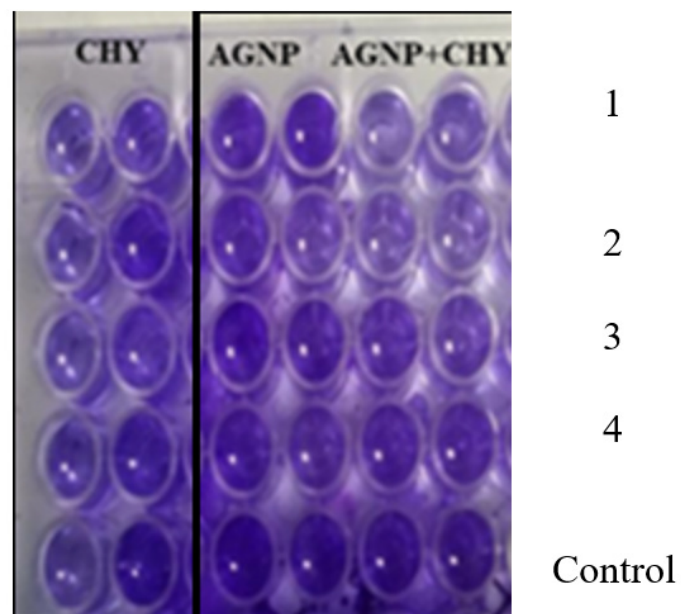


Figure 7: Rows (1-4 and control) of microtiter plates stained with crystal violet demonstrating biofilm adherence on the wall at concentrations ranging from 50, 25, 12.5, and 6.25 $\mu\text{g mL}^{-1}$ for chrysin (marked as CHY); 6.26, 3.13, 1.56 and 0.78 $\mu\text{g mL}^{-1}$ for silver nanoparticles (marked as AGNP) and 3.13, 1.56, 0.78, and 0.39 $\mu\text{g mL}^{-1}$ for nano-chrysin (marked as AGNP+CHY), and control.

sub-MIC values ranging from 3.13, 1.56, 0.78, and 0.39 $\mu\text{g mL}^{-1}$ with little adherence of biofilms on the walls of microtitre plate when washed and stained with crystal violet (Figures 6 and 7). Chrysin, in contrast, inhibited biofilm formation with very little effect at sub-MIC concentrations ranging from 50, 25, 12.5, and 6.25 $\mu\text{g mL}^{-1}$. Silver nanoparticles alone could not show potency as much as nano-chrysin with sub-MIC values ranging from 6.26, 3.13, 1.56 and 0.78 $\mu\text{g mL}^{-1}$. It is evident that chrysin and silver in the form of nano-chrysin prove to be very effective against antibiofilm activity (Figure 5a-c). Sub-MIC values of any effective compound induce stress and alter the expression of different bacterial genes.²⁸

DISCUSSION

The majority of bacterial pathogens use QS inhibition, which is a cutting-edge technique for identifying substances that might prove to be effective therapies for battling antibiotic resistance. Inhibition of biofilm formation is among those revolutionary methods.²⁹ As biofilm formation is governed by the LasR gene regulation, there have been several research studies done on the potential of polyphenols in inhibiting infections caused by *P. aeruginosa*.^{30,31} Bacterial cell clusters form biofilms when extracellular polysaccharide and glycoprotein matrix contains a network of internal channels or hollows that let the cells absorb nutrients and oxygen from the surrounding bulk liquid. Because they have a barrier preventing contact with antimicrobial agents, biofilms are more resistant to antimicrobials than bacteria.³¹ Studies show that polyphenols can effectively inhibit biofilm and function as an antibiotic substitute. Their mode of action includes blocking the matrix's formation, cell adhesion, and attachment, determining the generation of extracellular matrix, and reducing the production of virulence genes, all of which work together to inhibit biofilm formation.²⁷ For many years, plant bioactives have demonstrated effective defences against infections, and phytochemicals like Betulin, Betulinic acid, Chlorogenic acid, and Mosloflavone Cinnamic etc., all have potent anti-QS effects.³¹ In our study, we sought to determine whether natural polyphenol chrysin embedded in silver nanoparticles as nano-chrysin could prevent *P. aeruginosa* from forming biofilms that are controlled by quorum sensing signaling and the LasR gene. Characterization results showed nanoparticles formation, UV-vis showed SPR (Surface Plasmon Resonance) at 420 nm, indicating the reduction of silver by bioreductant chrysin without any harmful chemical use. The SPR phenomenon attributes to the size, dispersity and shape of nanoparticles exhibited in the colour variation at different stages of nanoparticle formation to generate brownish-yellow colour. When conducting electrons of metals interact with an electromagnetic field, they often fluctuate collectively in resonance with specific wavelengths. This phenomenon is known as surface plasmon resonance (SPR) and is observed in noble metal nanoparticles. The kind, size, form, and surroundings of the NPs profoundly influence these SPR bands. According to Dubey

et al. (2010),³² red shift in SPR spectra, a sign of polydispersity, occurred and NPs synthesized at greater metal ion concentration were larger. One O-H group, in the figure of FTIR of nano-chrysin coordinated the metal ions, as demonstrated by FTIR. The C=O oxygen atom, which was shifted to 1640 cm^{-1} in the spectra of the nano-chrysin complex and is therefore attributed to a strong band at about 1655 cm^{-1} that was found in the transmittance of the ligand, indicates that the crosslinking of ChR on metal NPs takes place through the C=O oxygen atom.⁴ After the reduction, differences in the transmittance intensity at 3500-3000 cm^{-1} are observed in the formulated nano-chrysin, which clearly illustrates the symmetrical and asymmetrical stretching modes of O-H, thus showing the loss of a single O-H group upon metal ion interaction. The morphological parameters obtained through SEM and HRTEM also indicated the size of the formed nanoparticles, with a minimum range of 2 nm. Additionally, it was discovered that the particles of nano-chrysin, which had a thin layer of chrysin coating on their surface, were evenly distributed and stable over an extended length of time. Since there is no evidence of direct particle contact, the capping agent's presence is mostly accountable. According to XRD data, nano-chrysin, which had a thin coating of chrysin on its surface, had well-dispersed particles with a minimum particle size of 2 nm that remained stable for a long time.¹⁷ PDI data of Table 1 indicated the stability of the nano-chrysin dispersion of the particles throughout the sample solution with a value of 0.26 which is fairly good value for nanoparticle formulation for drug delivery approaches.²⁵ Figures 6 and 7 shows that nano-chrysin exhibits significant potency and effectiveness in inhibiting biofilm formation. With sub-MIC concentrations ranging from 3.13, 1.56, 0.78, and 0.39 $\mu\text{g mL}^{-1}$, this nanoparticle was evaluated for antimicrobial assay, MIC, and inhibition of biofilm formation. Chrysin, in contrast, had little impact on biofilm formation at sub-MIC concentrations of 50, 25, 12.5, and 6.25 $\mu\text{g mL}^{-1}$. Silver nanoparticles by themselves could not match nano-chrysin sub-MIC, having ranges of sub-MIC 6.26, 3.13, 1.56, and 0.78 $\mu\text{g mL}^{-1}$ in terms of potency and efficacy. Hence, from our present study, it is evident that the combination of chrysin and silver nanoparticles, known as nano-chrysin, is very effective at preventing the growth of biofilms.

CONCLUSION

Since chrysin acts as a bioreductant to the silver metal ion, converting it from Ag^+ to Ag^0 , natural polyphenol chrysin has been used to produce nano-chrysin without the need of hazardous chemicals. We report in our research work that the generated silver nanoparticles can be utilized as an inhibitory agent to stop QS from being harmful, particularly from forming biofilms Figures 5 and 6. Antibiotic resistance is facilitated by biofilms, which also serve as a barrier to ligand entrance. By interfering with the LasR-mediated QS signaling pathway, which is in charge of biofilm formation, nano-chrysin disrupts the biofilm cascade and permits the entry of silver nanoparticles laden with chrysin,

which in turn stops the biofilm from forming. Nano-chrysin can be used in pre-clinical research and clinical trials to evaluate QS-mediated actions caused by *P. aeruginosa*, a pathogen that is cause for alarm, particularly in community-acquired infections that have nearly become resistant to most antibiotics, according to the results of the antibiofilm assay.

ACKNOWLEDGEMENT

All the lab work and drafting manuscript is done by Arnica F Lal that was checked by Dr. Pushpraj S Gupta.

CONFLICT OF INTEREST

The authors declare that there is no conflicts of interest.

ABBREVIATIONS

P. aeruginosa: *Pseudomonas aeruginosa*; **QS:** Quorum sensing; **Chrysin@AgNPs:** Nano-chrysin; **HRTEM:** High resolution transmission electron microscope; **XRD:** X-ray diffraction; **MIC:** Minimum inhibitory concentration; **PBS:** Phosphate buffered saline.

REFERENCES

1. Moradali MF, Ghods S, Rehm BH. *Pseudomonas aeruginosa* lifestyle: a paradigm for adaptation, survival, and persistence. *Front Cell Infect Microbiol*. 2017; 7: 39. doi: 10.3389/fcimb.2017.00039, PMID 28261568.
2. Bassetti M, Vena A, Croxatto A, Righi E, Guery B. How to manage *Pseudomonas aeruginosa* infections. *Drugs Context*. 2018; 7: 212527. doi: 10.7573/dic.212527, PMID 29872449.
3. Ventola CL. The antibiotic resistance crisis: part 1: causes and threats. *Pharm Ther*. 2015; 40(4): 277-83. PMID 25859123.
4. Shukla R, Pandey V, Vadnere GP, Lodhi S. Role of flavonoids in management of inflammatory disorders. In: *Bioactive food as dietary interventions for arthritis and related inflammatory diseases*. Academic Press Inc; 2019. p. 293-322.
5. Li AN, Li S, Zhang YJ, Xu XR, Chen YM, Li HB. Resources and biological activities of natural polyphenols. *Nutrients*. 2014; 6(12): 6020-47. doi: 10.3390/nu6126020, PMID 25533011.
6. Gao S, Siddiqui N, Etim I, Du T, Zhang Y, Liang D. Developing nutritional component chrysin as a therapeutic agent: bioavailability and pharmacokinetics consideration, and ADME mechanisms. *Biomed Pharmacother*. 2021; 142: 112080. doi: 10.1016/j.biopharm.2021.112080. PMID 34449320, PMCID PMC8653576.
7. Samarghandian S, Farkhondeh T, Azimi-Nezhad M. Protective effects of chrysin against drugs and toxic agents. *Dose-Response*. 2017; 15(2): 1559325817711782. doi: 10.1177/1559325817711782, PMID 28694744.
8. Yetisgin AA, Cetinel S, Zuvin M, Kosar A, Kutlu O. Therapeutic nanoparticles and their targeted delivery applications. *Molecules*. 2020; 25(9): 2193. doi: 10.3390/molecules 25092193, PMID 32397080.
9. Preda VG, Săndulescu O. Communication is the key: biofilms, quorum sensing, formation and prevention. *Discoveries (Craiova)*. 2019; 7(3): e100. doi: 10.15190/d.2019.13, PMID 32309618.
10. Lal AF, Singh S, Franco FC. Jr., Bhatia S. Potential of polyphenols in curbing quorum sensing and biofilm formation in Gram-negative pathogens. *Asian Pac J Trop Biomed*. 2021; 11(6): 231-43. doi: 10.4103/2221-1691.314044.
11. Wang J, Song M, Pan J, Shen X, Liu W, Zhang X, et al. Quercetin impairs *Streptococcus pneumoniae* biofilm formation by inhibiting sortase A activity. *J Cell Mol Med*. 2018; 22(12): 6228-37. doi: 10.1111/jcmm.13910, PMID 30334338.
12. Krishnan T, Yin WF, Chan KG. Inhibition of quorum sensing-controlled virulence factor production in *Pseudomonas aeruginosa* PAO1 by Ayurveda spice clove (*Syzygium aromaticum*) bud extract. *Sensors (Basel)*. 2012; 12(4): 4016-30. doi: 10.3390/s12040416, PMID 22666015.
13. Singh S, Datta S, Narayanan KB, Rajnish KN. Bacterial exo-polysaccharides in biofilms: role in antimicrobial resistance and treatments. *J Genet Eng Biotechnol*. 2021; 19(1): 140. doi: 10.1186/s43141-021-00242-y, PMID 34557983.
14. Tuon FF, Dantas LR, Suss PH, Tasca Ribeiro VS. Pathogenesis of the *Pseudomonas aeruginosa* biofilm: a review. *Pathogens*. 2022; 11(3): 300. doi: 10.3390/pathogens11030300, PMID 35335624.
15. Lee J, Zhang L. The hierarchy quorum sensing network in *Pseudomonas aeruginosa*. *Protein Cell*. 2015; 6(1): 26-41. doi: 10.1007/s13238-014-0100-x, PMID 25249263.
16. Eleraky NE, Allam A, Hassan SB, Omar MM. Nanomedicine fight against antibacterial resistance: an overview of the recent pharmaceutical innovations. *Pharmaceutics*. 2020; 12(2): 142. doi: 10.3390/pharmaceutics12020142, PMID 32046289.
17. Sathishkumar G, Bharti R, Jha PK, Selvakumar M, Dey G, Jha R, et al. Dietary flavone chrysin (5, 7-dihydroxyflavone ChR) functionalized highly-stable metal nanoformulations for improved anticancer applications. *RSC Adv*. 2015; 5(109): 89869-78. doi: 10.1039/C5RA15060D.
18. Luangtongkum T, Morishita TY, El-Tayeb AB, Ison AJ, Zhang Q. Comparison of antimicrobial susceptibility testing of *Campylobacter* spp. by the agar dilution and the agar disk diffusion methods. *J Clin Microbiol*. 2007; 45(2): 590-4. doi: 10.1128/JC.00986-06, PMID 17122005.
19. Rondevaldova J, Novy P, Urban J, Kokoska L. Determination of anti-staphylococcal activity of thymoquinone in combinations with antibiotics by checkerboard method using EVA capmat™ as a vapor barrier. *Arab J Chem*. 2017; 10(4): 566-72. doi: 10.1016/j.arabjc.2015.04.021.
20. Mahmoud MF, Fathy FM, Gohar MK, Soliman MH. Biofilm formation and quorum sensing lasR gene of *Pseudomonas aeruginosa* isolated from patients with post-operative wound infections. *Eur J Mol Clin Med*. 2021; 8(2): 2177-89.
21. Shankar SS, Rai A, Ahmad A, Sastry M. Rapid synthesis of Au, Ag, and bimetallic Au core-Ag shell nanoparticles using Neem (*Azadirachta indica*) leaf broth. *J Colloid Interface Sci*. 2004; 275(2): 496-502. doi: 10.1016/j.jcis.2004.03.003, PMID 15178278.
22. Kasthuri J, Veerapandian S, Rajendiran N. Biological synthesis of silver and gold nanoparticles using apii as reducing agent. *Colloids Surf B Biointerfaces*. 2009; 68(1): 55-60. doi: 10.1016/j.colsurfb.2008.09.021, PMID 18977643.
23. Li S, Shen Y, Xie A, Yu X, Qiu L, Zhang L, et al. Green synthesis of silver nanoparticles using *Capsicum annuum* L. extract. *Green Chem*. 2007; 9(8): 852-8. doi: 10.1039/b615357g.
24. Philip D, Unni C, Aromal SA, Vidhu VK. *Murraya Koenigii* leaf-assisted rapid green synthesis of silver and gold nanoparticles. *Spectrochim Acta A Mol Biomol Spectrosc*. 2011; 78(2): 899-904. doi: 10.1016/j.saa.2010.12.060, PMID 21215687.
25. Clarke S. Dublin City University; northside, Dublin [Ph.D. thesis]; 2013. Development of Hierarchical Magnetic Nanocomposite Materials for Biomedical Applications.
26. Ahmadi K, Hashemian AM, Bolvardi E, Hosseini PK. Vancomycin-resistant *Pseudomonas aeruginosa* in the cases of trauma. *Med Arch*. 2016; 70(1): 57-60. doi: 10.5455/medarh.2016.70.57-60, PMID 26980934.
27. Qin S, Xiao W, Zhou C, Pu Q, Deng X, Lan L, et al. *Pseudomonas aeruginosa*: pathogenesis, virulence factors, antibiotic resistance, interaction with host, technology advances and emerging therapeutics. *Signal Transduct Target Ther*. 2022; 7(1): 199. doi: 10.1038/s41392-022-01056-1, PMID 35752612.
28. Narimisa N, Amraei F, Kalani BS, Mohammadzadeh R, Jazi FM. Effects of sub-inhibitory concentrations of antibiotics and oxidative stress on the expression of type II toxin-antitoxin system genes in *Klebsiella pneumoniae*. *J Glob Antimicrob Resist*. 2020; 21: 51-6. doi: 10.1016/j.jgar.2019.09.005, PMID 31520807.
29. Sharma S, Mohler J, Mahajan SD, Schwartz SA, Bruggemann L, Aalinkeel R. Microbial biofilm: a review on formation, infection, antibiotic resistance, control measures, and innovative treatment. *Microorganisms*. 2023; 11(6): 1614. doi: 10.3390/microorganism 11061614, PMID 37375116, PMCID PMC10305407.
30. Roy R, Tiwari M, Donelli G, Tiwari V. Strategies for combating bacterial biofilms: A focus on anti-biofilm agents and their mechanisms of action. *Virulence*. 2018; 9(1): 522-54. doi: 10.1080/21505594.2017.1313372, PMID 28362216, PMCID PMC5955472.

Cite this article: Lal AF, Gupta PS. An Exploration of Chrysin Fabricated Silver Nanoparticles as Antibiofilm Agent against *Pseudomonas aeruginosa*. *Indian J of Pharmaceutical Education and Research*. 2024;58(2s):s429-s435.